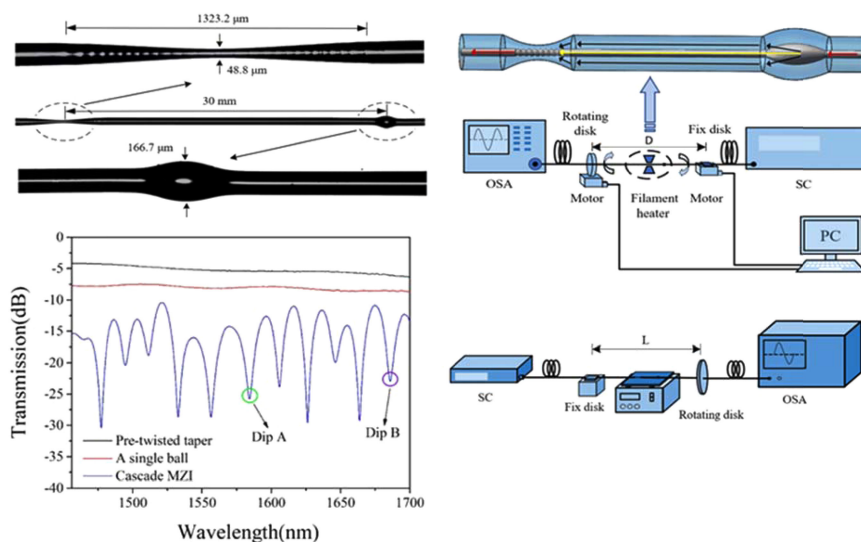


High Sensitive Directional Twist Sensor Based on a Mach–Zehnder Interferometer

Volume 10, Number 6, December 2018

Shujie Duan
Weiliang Liu
Cuiting Sun
Hang Jiang
Chong Yao
Kai Zhang
Xingyu Bai
Wen Wang
Cunlian Lu
Tao Geng
Feng Peng
Libo Yuan



DOI: 10.1109/JPHOT.2018.2880450

1943-0655 © 2018 IEEE

High Sensitive Directional Twist Sensor Based on a Mach–Zehnder Interferometer

Shujie Duan,¹ Weiliang Liu,¹ Cuiting Sun ,¹ Hang Jiang,¹
Chong Yao,¹ Kai Zhang,¹ Xingyu Bai,¹ Wen Wang,¹ Cunlian Lu,¹
Tao Geng ,¹ Feng Peng ,² and Libo Yuan ³

¹Key Laboratory of In-Fiber Integrated Optics, Ministry Education of China, College of Science, Harbin Engineering University, Harbin 150001, China

²School of Physics and Technology, University of Jinan, Jinan 250022, China

³Photonics Research Center, Guilin University of Electronics Technology, Guilin 541004, China

DOI:10.1109/JPHOT.2018.2880450

1943-0655 © 2018 IEEE. Translations and content mining are permitted for academic research only.

Personal use is also permitted, but republication/redistribution requires IEEE permission.

See http://www.ieee.org/publications_standards/publications/rights/index.html for more information.

Manuscript received September 15, 2018; revised October 28, 2018; accepted November 5, 2018. Date of publication November 9, 2018; date of current version November 20, 2018. This work was supported in part by the National Nature Science Foundation of China under Grants 61377084, 41174161, and 61775044; in part by the Joint Research Fund in Astronomy under Grant U1631239 under cooperative agreement between the National Natural Science Foundation of China and the Chinese Academy of Sciences (CAS); in part by the Opening Project of Key Laboratory of Astronomical Optics and Technology, Nanjing Institute of Astronomical Optics and Technology, CAS under Grants CAS-KLAOT-KF201501 and CAS-KLAOT-KF201605; and in part by the Aeronautical Science Foundation of China under Grant 201608P6003. Corresponding authors: Tao Geng and Feng Peng (e-mail: gengtao_hit_oe@126.com; pengfeng8283@163.com).

Abstract: A new type of Mach–Zehnder interferometer (MZI) is proposed to measure twist and temperature. The sensor contains a pretwisted taper and a ball. The pretwisted taper is made by pretwisted, and then, thermally tapering along a single-mode fiber, to induce permanent spiral distortion in the fiber. The experimental results indicate that the sensor has higher twist sensitivity. Twisting the sensor for counterclockwise and clockwise direction, the twist sensitivities of Dip 1584 nm are -0.378 and 0.083 nm/(rad/m), respectively, and the twist sensitivities of Dip 1685 nm are -0.117 and 0.089 nm/(rad/m), respectively. Meanwhile, the twist direction can be determined by the value of the twist sensitivities. The temperature sensitivities of Dip 1584 and Dip 1685 nm are 63 pm/°C and 74 pm/°C, respectively. The feasibility of measuring the torsion and temperature characteristics has been experimentally confirmed. Thus, the proposed MZI sensor can be used to measure twist and temperature and discriminate twist direction.

Index Terms: Mach–Zehnder interferometer, temperature, twist, pre-twisted taper.

1. Introduction

In recent years, due to the application of external torque, the research on twist, twist angle and twist sensors has been developed rapidly, such as bridge safety monitoring, biochemical sensing and power system monitoring [1], [2]. Many twist sensors play an important position in these fields, but there are many shortcomings in their applications. For example, the mechanical twist sensor requires higher cost and machining requirements, and the electromagnetic twist sensor is large in volume and vulnerable to electromagnetic interference. Therefore, using the optical fiber sensor provides another option for twist measurement, because of its small volume and light wave frequency selection. Many different fiber gratings are used as twist sensors, such as CO₂

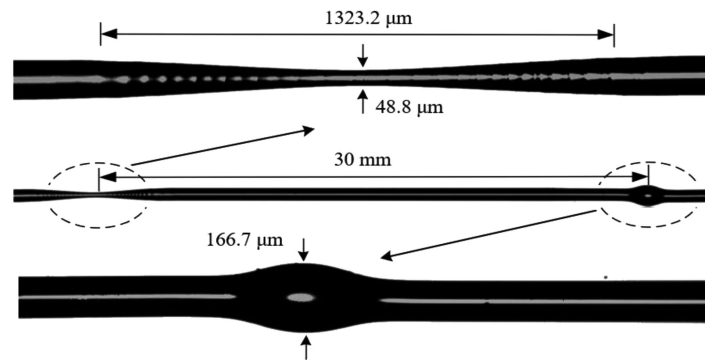


Fig. 1. Structural parameters and side visibility.

laser internal long period fiber gratings (LPFGs) [3]–[6] and fiber Bragg gratings (FBGs) [7]–[9]. In addition, Mach-Zehnder interferometer (MZI) is also used as fiber twist sensor, such as the tapered fiber Mach-Zehnder interferometers (TFMZIs) [10], the pre-twisted in-fiber MZI (PT-MZI) [11], the abrupt-tapered Mach-Zehnder interferometers (AT-MZI) [12], and the in-line optical fiber MZI [13]. However, some sensors are unable to distinguish the twist directions, or have a lower sensitivity, or require the more special materials. In a single-mode fiber, a twisted structure responds better to its twist characteristic. For a linear state of polarization (SOP), the twist of the fiber is linear with the polarization state because the birefringence occurs on the fibers. Based on R. Ulrich *et al.* first theoretically proposed that the polarization of light in a twisted single-mode fiber (SMF) is influenced by the strain-induced optical activity of the rotating processes [14].

In this paper, a twist MZI sensor is presented to improve the twist sensitivity and discriminate the direction of twist. The sensor is made by connecting a simple ball and a pre-twisted taper together. Meanwhile, the principle of torsion characteristic is also described in detail. The experimental results show that the twist sensitivities will change in different twist direction. Through the analysis of experimental results, the MZI sensor can accomplish twist measurement with much higher sensitivity and the discrimination of twist direction. Furthermore, the temperature measurement is also presented in the article.

2. Fabrication Set-Up and Characteristics of Spectra

As shown in Fig. 1, the sensor was made by cascading a pre-twisted taper and a small ball. The taper waist diameter is $48.8 \mu\text{m}$ and the twist length is $1323.2 \mu\text{m}$ and the ball diameter is $166.7 \mu\text{m}$. The distance between them is about 30 mm.

The schematic diagram of manufacturing device for the pre-twisted taper is shown in Fig. 2. It can be seen from this figure, the experimental processes were described as follows: At first, a single-mode fiber was fixed between two motors, a rotating disc was placed on one motor to provide twist into the fiber. And the fiber was rotated for 20 revolutions by turning the rotating disc. Simultaneously, the filament heater was used to soften the fiber and make sure the fiber can be generated the permanent spiral distortion, when the filament heater power is about 53 w, the center temperature reaches the working temperature of $1200 \text{ }^\circ\text{C}$, This type of the filament heater has a width of 1 mm. Then, through handling two motors, which are controlled by a personal computer (PC) to make the fiber tapered because of the difference in speed of them. The fiber was stretched as taper during torsion recovery, with the filament heater working continuously at the same time. Lastly, the pre-twisted taper and the small ball together form the MZI sensor. The distance between two motors is approximately $D = 262 \text{ mm}$.

As shown in Fig. 3, the interference phenomenon only occurs in cascade MZI compared to a single pre-twist taper and a single ball. In this study, the Dip 1584 nm and Dip 1685 nm (Dip A and Dip B) with higher fringe visibility are chosen as the research peak. And it is found that the Dip

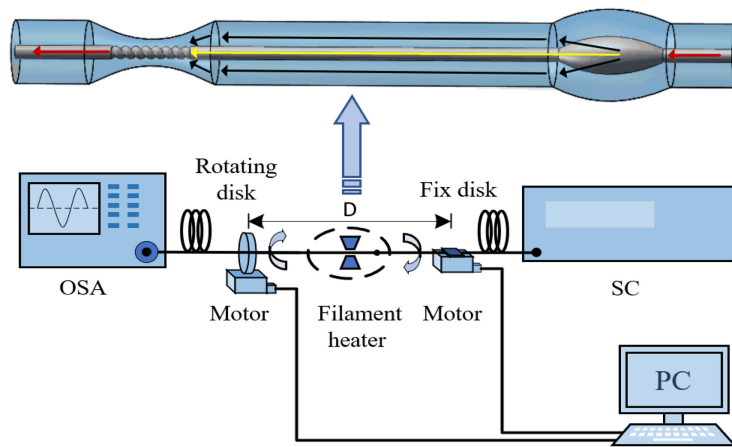


Fig. 2. Schematic diagram of pre-twisted taper and its manufacturing device.

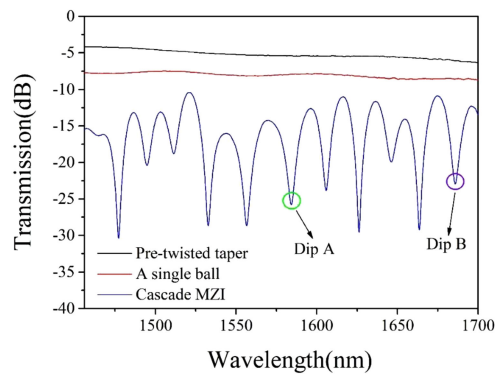


Fig. 3. Pre-twist, small ball and cascade of MZI's Spectrum.

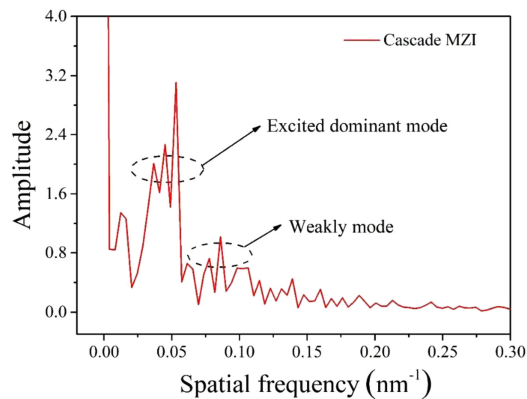


Fig. 4. Spatial frequency spectrum of the MZI sensor.

1584 nm and Dip 1685 nm of the cascade MZI is blue-shifted or red-shifted with changes in twist rate and temperature. Meanwhile, a fast Fourier transformed (FFT) is achieved on the transmission spectrum of the cascade MZI with the FFT- spatial frequency spectra to provide a deep sight into the mode components involved in the interference process in Fig. 4. It can be seen that the interference figure contains more than three modes (the dominant mode and the weakly mode), and the sensor can generate the interference between the fiber core mode and the cladding mode of the structure

[1]. The spectra are inhomogeneous because more than two modes are involved in the interference process, some else cladding modes are generated, which changes the envelope of the interference spectrum [15].

3. Experimental Principle

As shown in Fig. 2, when the input light propagates into the ball (rad arrow), some of the cladding modes with different effective refractive indices may be excited (black arrow) [16], and the remaining light still propagates in the core as the fundamental core mode (yellow arrow). Then, with light is input into a pre-twisted taper, its core follows a helicoidal path inside the cladding, and its polarization rotates during the propagation processes. The cladding modes are recoupled back into the pre-twist taper, this structure reaches the condition that constitutes the MZI. The twist is induced by shear strain in a SMF because of the photo-elastic effect [15], [17]. The torsion plays an important role in this structure. For example, when an ordinary single-mode fiber is rotated, it can occur permanent spiral distortion. And even a slight rotation is enough to shift the wavelength [18]. In addition, a pre-twisted MZI based on an ordinary single-mode fiber can research the torsion characteristics and discriminate the direction of twist [11]. Thus, it was proved that the torsion can not only improve the twist sensitivity but also distinguish the direction. Meanwhile, the role of the taper is also indispensable. In TFMZIs, the spectral sensitivity of the proposed tapered-based twist sensor would depend on the structure of the fiber taper and the thin waist might have a higher sensitivity [10]. Therefore, the taper exists in the proposed structure. Furthermore, due to the symmetry of the ball, the ball satisfies the condition of MZI in the structure and does not affect the torsional characteristics. It can better study the torsional characteristics of the pre-twisted taper on the sensor.

The light polarization can also rotate in a helicoidal fiber due to the fiber's geometric rotation [19]. Moreover, in the paraxial region, the speed of rotation of cladding modes is not different from the core mode in a twisted fiber [20]. However, when portion of the light in the cladding is coupled into the fiber core after by fiber cross section between a pre-twisted taper and a ball, where portion of the light is attenuated because of cladding mode propagation. The propagation constant of the fiber core is not same as the cladding mode, so the modes propagate at different speeds. In addition, the modes produce a phase difference when passing through the fiber structure. The intensity transfer function can be derived as a two-mode interferometer [21].

$$I = I_{co} + I_{cl} + 2\sqrt{I_{co}I_{cl}}\cos\varphi \quad (1)$$

where I_{co} and I_{cl} are the intensities of light guided in the fiber core and cladding modes, respectively, and $\varphi = (2\pi\Delta n_{eff}L_0)/\lambda$ is the phase difference between the different modes, where λ is the used wavelength, L_0 is the interference distance which is about equal to L , and $\Delta n_{eff} = n_{eff}^{co} - n_{eff}^{cl}$ is the difference between the effective refractive indices of the core n_{eff}^{co} and cladding n_{eff}^{cl} modes. When the phase difference $\varphi = (2m + 1)\pi$, $m = 0, 1, 2, \dots$, the transmission dips appear in

$$\lambda_m = \frac{2L\Delta n_{eff}}{2m + 1} \quad (2)$$

where λ_m is the central wavelength of the m th order interference dip. The interference fringe spacing between adjacent interference gaps about is $FSR \approx \lambda_m^2/(\Delta n_{eff}L)$. In this paper, the MZI sensor can response to external variables through investigating changes in wavelength.

When the sensor suffer from shear strain, from Eq. (2) and the effect of the variable L can be ignored, the wavelength change can be expressed as

$$\Delta\lambda_m \approx \lambda_m \frac{\delta\Delta n_{eff}}{\Delta n_{eff}} \quad (3)$$

where $\delta\Delta n_{eff}$ is the variable of Δn_{eff} , which is induced by the birefringence due to the photo-elastic effect. $\delta\Delta n_{eff} = (g^{co}n_{eff}^{co} - g^{cl}n_{eff}^{cl})\tau$ is linearly proportional to the twist rate τ , g^{co} and g^{cl} the photo-elastic constants for fiber core and cladding material, respectively. Thus, $\Delta\lambda_m$ in response to twist

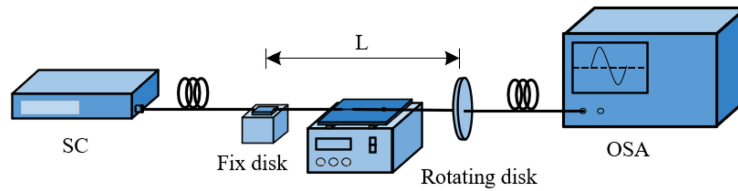


Fig. 5. Experimental set-up of twist and temperature measurement.

τ can be derived as [11]

$$\Delta\lambda_m = \frac{\lambda_m}{\Delta n_{eff}} (g^{co} n_{eff}^{co} - g^{cl} n_{eff}^{cl}) \tau \quad (4)$$

where the term of $\lambda_m(g^{co} n_{eff}^{co} - g^{cl} n_{eff}^{cl})/\Delta n_{eff}$ is a wavelength-independent constant, therefore, the wavelength shift $\Delta\lambda_m$ is linearly proportional to the twist rate τ .

Obviously, when the twist MZI sensor having birefringence was twisted, the twist-induced shearing stress resulted in birefringence by means of the photo-elastic effect, which made $\delta\Delta n_{eff}$ increase or decrease [14]. According to Equation 4, the change of $\delta\Delta n_{eff}$ resulted in the Dip 1584 nm and Dip 1685 nm shifting ($\Delta\lambda_m$) when the twist MZI sensor was twisted. The magnitude of the $\Delta\lambda_m$ change determines the absolute value of the twist sensitivity. In addition to, the twist-induced birefringence is proportional to the twist rate, and the direction of the birefringence vector is determined by the twist direction [14]. That is, right-rotatory birefringence is induced as the twist MZI sensor is twisted clockwise, whereas left-rotatory birefringence is induced as it is twisted counterclockwise. Furthermore, right- or left-rotatory birefringence results in $\delta\Delta n_{eff}$ changing oppositely, i.e., increasing or decreasing. Therefore, the Dip 1584 nm and Dip 1685 nm shifted linearly towards longer wavelength (red shift) as the twist MZI sensor was twisted clockwise, and the opposite process occurred (blue shift) as the twist MZI sensor was twisted counterclockwise. Thus, this twist MZI sensor can measure the twist and discriminate the twist direction simultaneously.

4. Experimental Results and Discussions

As shown in Fig. 5, the experimental measuring set-up is used to demonstrate that the MZI sensor can measure torsion characteristics. The MZI sensor is held between a fixed disk and a rotating disk which can turn the sensor counterclockwise and clockwise direction. The distance between two stages is $L = 170$ mm. At the same time, a heating device is added under the MZI sensor. One end of the MZI sensor is connected to the Super-continuum Light Source (SLS), and the other end is connected to Optical Spectrum Analyzer (OSA) to record spectra simultaneously. The resolution of the OSA is set to 0.2 nm and the wavelength range used in experiments is 1450 nm~1700 nm. Therefore, the twist measurement can be finished by turning the rotating disk. Meanwhile, by heating the heating apparatus for different ambient temperature, the temperature measurement of the sensor can be achieved.

Figs. 6(a) and (b) are shown the Dip 1584 nm and Dip 1685 nm shift versus twist rate. In the measurement of torsion characteristics, the twist angle is measured every $\pi/9$ within the twist range of $-\pi \sim \pi$ (counterclockwise (-) and clockwise (+) direction). It can be seen from Fig. 6(a) and (b), the wavelength shift is sensitive to the direction of twist, as indicated by the wavelength shifts exhibiting an opposite response to the application of counterclockwise and clockwise torsions, corresponding to a blue shift and red shift, respectively. The wavelength shift is approximately linearly proportional to the twist rate in both counterclockwise and clockwise directions. After the data is linearly fitted, we conclude that the twist sensitivities of Dip 1584 nm are -0.378 nm/(rad/m) and 0.083 nm/(rad/m), respectively. And Dip 1685 nm are -0.117 nm/(rad/m) and 0.089 nm/(rad/m), respectively.

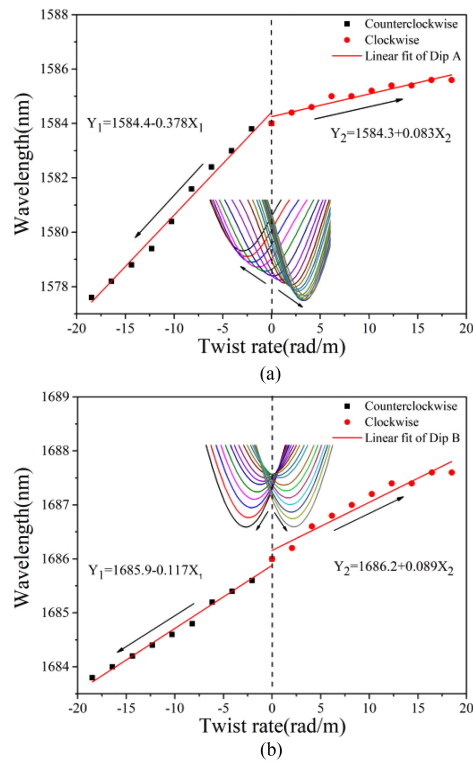


Fig. 6. The torsion characteristics for cascade MZI. (a) Enlarged drawing and twist characteristics measurement of Dip A. (b) Enlarged drawing and twist characteristics measurement of Dip B. of the experimental setup.

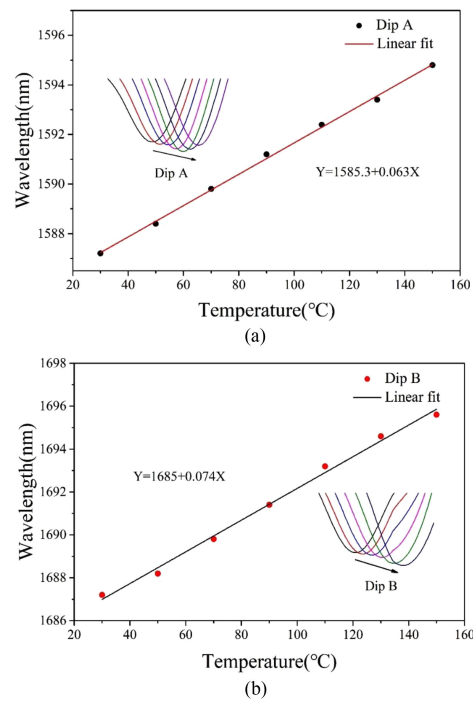


Fig. 7. The temperature characteristics for cascade MZI. (a) Enlarged drawing and temperature characteristics measurement of Dip A. (b) Enlarged drawing and temperature characteristics measurement of Dip B.

The temperature characteristics of Dip 1584 nm and Dip 1685 nm were also studied to determine if the proposed sensor had a favorable effect on the temperature. The temperature was changed once every 20 °C (30~150 °C), and the OSA was used to record temperature characteristics data at a time. It can be seen from Figs. 7(a) and (b), as the temperature continues to increase, the wavelengths at Dip 1584 nm and Dip 1685 nm have a red shift. And the temperature sensitivities of 1584 nm and 1685 nm are 63 pm/°C and 74 pm/°C, respectively.

5. Conclusion

A novel MZI sensor, based on a pre-twisted taper and a ball, is proposed and experimentally demonstrated to obtain the high twist sensitivity and to discriminate the twist direction. The results of the study indicate that the twist sensitivities of Dip 1584 nm are -0.378 nm/(rad/m) and 0.083 nm/(rad/m) in counterclockwise and clockwise direction, respectively, and the twist sensitivities of Dip 1685 nm are -0.117 nm/(rad/m) and 0.089 nm/(rad/m) in counterclockwise and clockwise direction, respectively. Meanwhile, the twist direction can be discriminated depending on the value of the twist sensitivity. Furthermore, the temperature sensitivities of Dip 1584 nm and 1685 nm are 63 pm/°C and 74 pm/°C, respectively. The sensor has been experimentally shown the feasibility in the field of torsion and temperature characteristics measurement.

References

- [1] C. Zhang, T. Ning, J. Li, J. J. Zheng, X. K. Gao, and L. Pei, "Refractive index and strain sensor based on twin-core fiber with a novel T-shaped taper," *Opt. Laser Technol.*, vol. 102, pp. 12–16, Jun. 2018.
- [2] L. A. Wang, C. Y. Lin, and G. W. Chern, "A torsion sensor made of a corrugated long period fibre grating," *Meas. Sci. Technol.*, vol. 12, no. 7, pp. 793–799, Apr. 2001.
- [3] X. Qiao, Y. Wang, and H. Yang, "Ultrahigh-temperature chirped fiber Bragg grating through thermal activation," *IEEE Photon. Technol. Lett.*, vol. 27, no. 12, pp. 1305–1308, Jun. 2015.
- [4] Y. P. Wang, J. P. Chen, and Y. J. Rao, "Torsion characteristics of long period fiber gratings induced by high-frequency CO₂ laser pulses," *J. Opt. Soc. Amer. B*, vol. 22, no. 6, pp. 1167–1172, Jun. 2005.
- [5] Y. J. Rao, Y. P. Wang, Z. L. Ran, and T. Zhu, "Novel fiber-optic sensors based on long-period fiber gratings written by high-frequency CO₂ laser pulses," *J. Lightw. Technol.*, vol. 21, no. 5, pp. 1320–1327, May 2003.
- [6] L. Y. Shao, A. P. Zhang, and W. S. Liu, "Optical refractive-index sensor based on dual fiber-Bragg gratings interposed with a multimode-fiber taper," *IEEE Photon. Technol. Lett.*, vol. 19, no. 1, pp. 30–32, Mar. 2007.
- [7] X. Shu, B. A. L. Gwandu, and Y. Liu, "Sampled fiber Bragg grating for simultaneous refractive-index and temperature measurement," *Opt. Lett.*, vol. 26, no. 11, pp. 774–776, Jun. 2001.
- [8] H. J. Patrick, A. D. Kersey, and F. Bucholtz, "Analysis of the response of long period fiber gratings to external index of refraction," *J. Lightw. Technol.*, vol. 16, no. 9, pp. 1606–1612, Sep. 1998.
- [9] J. F. Ding, A. P. Zhang, and L. Y. Shao, "Fiber-taper seeded long-period grating pair as a highly sensitive refractive-index sensor" *IEEE Photon. Technol. Lett.*, vol. 17, no. 6, pp. 1247–1249, May 2005.
- [10] C. M. Li, C. W. Chan, J. S. Horng, J. M. Hsu, and C. L. Lee, "Fiber-optic twist sensor based on a tapered fiber Mach-Zehnder interferometer," in *Proc. 10th Conf. Lasers Electro-Opt. Pacific Rim*, Kyoto, Japan, 2013, pp. 1–2.
- [11] Z. Y. Bai *et al.*, "Torsion sensor with rotation direction discrimination based on a pre-twisted in-fiber Mach-Zehnder interferometer," *IEEE Photon. J.*, vol. 9, no. 3, Jun. 2017, Art. no. 7103708.
- [12] G. L. Cheng, J. J. Wang, Z. Z. Feng, and N. K. Chen, "Simultaneous twist angle and direction sensing using abrupt-tapered fiber Mach-Zehnder interferometers," in *Proc. 6th Int. Conf. Sens. Technol.*, Kolkata, India, 2012, pp. 460–463.
- [13] Q. J. Fu *et al.*, "Intensity-modulated directional torsion sensor based on in-line optical fiber Mach-Zehnder interferometers," *Opt. Lett.*, vol. 43, no. 10, pp. 2414–2417, May 2001.
- [14] R. Ulrich and A. Simon, "Polarization optics of twisted single-mode fibers," *Appl. Opt.*, vol. 18, no. 13, pp. 2241–2251, Jul. 1979.
- [15] A. T. Zhu *et al.*, "Refractive index sensing based on Mach-Zehnder interferometer formed by three cascaded single-mode fiber tapers," *Appl. Opt.*, vol. 50, no. 11, pp. 1548–1533, Apr. 2011.
- [16] L. Jiang, J. Yang, S. Wang, B. Li, and M. Wang, "Fiber Mach-Zehnder interferometer based on microcavities for high-temperature sensing with high sensitivity," *Opt. Lett.*, vol. 36, no. 19, pp. 3753–3755, Oct. 2013.
- [17] A. M. Smith, "Birefringence induced by bends and twists in single-mode optical fiber," *Appl. Opt.*, vol. 19, no. 15, pp. 2606–2611, Aug. 2011.
- [18] O. V. Ivanov, "Fabrication of long-period fiber gratings by twisting a standard single-mode fiber," *Opt. Lett.*, vol. 30, no. 24, pp. 3290–3292, Dec. 2005.
- [19] F. Wassmann and A. Ankiewicz, "Berry's phase analysis of polarization rotation in helicoidal fibers," *Appl. Opt.*, vol. 37, no. 18, pp. 3902–3911, Jun. 1998.
- [20] O. V. Ivanov, "Propagation and coupling of hybrid modes in twisted fibers," *J. Opt. Soc. Amer. A, Opt. Image Sci. Vis.*, vol. 22, no. 4, pp. 716–723, Apr. 2005.
- [21] T. Wei, X. Lan, and H. Xiao, "Fiber inline core-cladding-mode Mach-Zehnder interferometer fabricated by two-point CO₂ laser irradiations," *IEEE Photon. Technol. Lett.*, vol. 21, no. 10, pp. 669–671, Jun. 2005.